The Plant Cell, Vol. 11, 1755–1767, September 1999, www.plantcell.org

MAF1, a Novel Plant Protein Interacting with Matrix Attachment Region Binding Protein MFP1, Is Located at the Nuclear Envelope

Frank Gindullis,[1] Nancy J. Peffer, and Iris Meier[2]

DuPont Central Research and Development, P.O. Box 80402, Wilmington, Delaware 19880-0402

The interaction of chromatin with the nuclear matrix via matrix attachment region (MAR) DNA is considered to be of fundamental importance for chromatin organization in all eukaryotic cells. MAR binding filament–like protein 1 (MFP1) from tomato is a novel plant protein that specifically binds to MAR DNA. Its filament protein–like structure makes it a likely candidate for a structural component of the nuclear matrix. MFP1 is located at nuclear matrix–associated, speckle-like structures at the nuclear envelope. Here, we report the identification of a novel protein that specifically interacts with MFP1 in yeast two-hybrid and in vitro binding assays. MFP1 associated factor 1 (MAF1) is a small, soluble, serine/threonine-rich protein that is ubiquitously expressed and has no similarity to known proteins. MAF1, like MFP1, is located at the nuclear periphery and is a component of the nuclear matrix. These data suggest that MFP1 and MAF1 are in vivo interaction partners and that both proteins are components of a nuclear substructure, previously undescribed in plants, that connects the nuclear envelope and the internal nuclear matrix.

INTRODUCTION

The nuclear matrix is a structural framework believed to be involved in the architectural organization of nucleic acid metabolism in the eukaryotic nucleus. Biochemically, the nuclear matrix is defined as the insoluble material that remains after removal of chromatin and soluble nuclear proteins (Berezney and Coffey, 1974; Mirkovitch et al., 1984). It appears as a network of ~10-nm fibers in electron micrographs. This network is reminiscent of the intermediate filament cytoskeleton (Nickerson et al., 1995). Although this filament-like structure depends on the preparation method and is still somewhat controversial (reviewed in Nickerson et al., 1995), more recent evidence has shown that the animal nuclear matrix contains protein complexes involved in transcription, splicing, and replication (Misteli and Spector, 1998; Wei et al., 1998), indicating that it may play an important role in the functional compartmentalization of these nuclear processes.

The animal nuclear matrix consists of two parts, the nuclear lamina, which is a meshwork of filaments that line the inner surface of the nuclear envelope, and the internal nuclear matrix (Nickerson et al., 1995). Although no structural components of the internal nuclear matrix have been isolated from any organism, the nuclear lamina is relatively well characterized. It consists primarily of the nuclear lamins A, B, and C, which are proteins that structurally are closely related to the intermediate filament proteins of the cytoplasmic cytoskeleton. Like intermediate filament proteins, lamins consist of globular head and tail domains, which are connected by a long α-helical coiled-coil domain (McKeon et al., 1986). Lamins have been found to bind to matrix attachment region (MAR) DNA as well as to histones and intact chromatin (Luderus et al., 1992; Taniura et al., 1995). They are believed to be involved in attaching chromatin to the nuclear envelope of the interphase nucleus as well as to be important in the orchestration of daughter nuclei formation during cytokinesis (Gant and Wilson, 1997).

Despite some earlier efforts to identify plant lamins (Beven et al., 1991; McNulty and Saunders, 1992; Minguez and Moreno Diaz de la Espina, 1993), no such proteins have been cloned or purified from plants. Because the fully sequenced yeast genome does not contain lamin-encoding genes (Mewes et al., 1998), it is conceivable that different proteins might have evolved in nonanimal eukaryotes that functionally replace the animal nuclear lamins.

MAR binding filament–like protein 1 (MFP1) was isolated by functional cloning from tomato. MFP1 was the first plant protein shown to bind specifically to MARs and to be a component of the plant nuclear matrix (Meier et al., 1996). Like lamins, MFP1 contains an extended α-helical coiled-coil domain, but it has no globular head and tail domains. MFP1 has weak sequence similarity to cytoplasmic and nuclear

[1] Current address: Institute of Crop Science and Plant Breeding, Christian Albrechts University of Kiel, Olshausenstrasse 40, D-24118 Kiel, Germany.

[2] To whom correspondence should be addressed. E-mail meieri@esvax.dnet.dupont.com; fax 302-695-4296.

filament proteins from animals and yeast, such as myosin heavy chain, tropomyosin, and nuclear mitotic apparatus protein (Meier et al., 1996). Its predicted structure and sequence similarity suggest that MFP1 may be capable of forming filaments, a property that makes it a good candidate for a structural protein of a plant nuclear skeleton.

Two functional domains of MFP1 have been identified. A C-terminal domain of 228 amino acids, which is part of the coiled-coil domain, is necessary and sufficient for MAR binding (Meier et al., 1996). An N-terminal domain of 125 amino acids diverges structurally from the coiled-coil domain and contains two hydrophobic regions, one of which has similarity to several transmembrane domains (Meier et al., 1996). This 125–amino acid domain is required for the specific targeting of MFP1 to specklelike structures at the nuclear envelope, which are associated with the nuclear matrix (Gindullis and Meier, 1999). Hence, MFP1 is a novel candidate in plants for a protein that connects chromatin with the nuclear envelope and, due to its filament-like structure, possibly to elements of the nuclear skeleton.

Many coiled-coil proteins have been shown to be involved in protein–protein interactions, both by homodimerization and heterodimerization of the coiled-coil domains and by interactions with structurally dissimilar proteins. The nuclear lamins bind both to each other, forming the lamina, and to at least two structurally different proteins of the inner nuclear membrane. These proteins most likely anchor the lamina to the nuclear envelope (Simos and Georgatos, 1992; Foisner and Gerace, 1993). In an attempt to identify additional potential components of the undescribed plant nuclear skeleton–nuclear envelope complex, we have used MFP1 in a yeast two-hybrid screen. Here, we report the identification of a novel protein that specifically interacts with MFP1 and that is, like MFP1, located at the plant nuclear envelope and is a component of the nuclear matrix.

RESULTS

Screening of a Tomato Two-Hybrid Library for Proteins That Interact with MFP1

Figure 1A shows a schematic representation of tomato MFP1. It has been shown that the N-terminal domain, containing two stretches of hydrophobic amino acids, is involved in targeting MFP1 to a specific subdomain of the nuclear periphery (Gindullis and Meier, 1999). The MAR binding domain is located within the C-terminal 228 amino acids (Meier et al., 1996). For the yeast two-hybrid screen, a subfragment of MFP1 from amino acid 83 to amino acid 491 (HHMFP1) was used to construct the bait plasmid pBD–HHMFP1 (Figure 1A). This fragment was chosen to prevent both targeting of the bait protein to the nuclear periphery and competition for DNA binding of the MAR binding domain with the GAL4 DNA binding domain of the bait protein. HHMFP1 contains the majority of the α-helical coiled-coil domain of MFP1, predicted to be involved in protein–protein interactions. Δ125HMFP1 (Figure 1A) is a second subfragment of MFP1 tested in the yeast two-hybrid assay. It is identical to HHMFP1, except that it lacks both hydrophobic domains. A third subfragment, Δ125MFP1, lacks the hydrophobic domains but contains the DNA binding domain. This MFP1 subfragment was overexpressed in a baculovirus expression system and used for protein overlay experiments (see Figure 1E).

The yeast strain YRG-2, containing two reporter genes (*lacZ* and *HIS3*), was cotransformed with pBD–HHMFP1 and a two-hybrid library from young tomato leaves, and 1×10^6 transformants were plated on His^-, Leu^-, and Trp^- selection plates (synthetic complete media without His, Leu, and Trp). Transformants growing on these plates were screened for β-galactosidase activity, and plasmids giving rise to the expression of both reporter genes were retransformed together with the bait plasmid and tested again for growth on His^-, Leu^-, and Trp^- selection plates and for β-galactosidase activity in filter lift assays. The three plasmids pAD6-3, pAD21-1, and pAD40-1 scored positive for both reporter genes after retransformation. Sequencing of the inserts showed that the three cDNAs encoded an identical protein sequence in frame with the GAL4 DNA binding domain. The deduced protein was named MAF1 (for MFP1 associated factor 1). The cDNA inserts had sizes of 709 bp for pAD21-1 and pAD40-1 and 690 bp for pAD6-3.

The specificity of interaction with the bait protein was tested for pAD21-1, as shown in Figure 1B. Yeast YRG-2 cells were cotransformed with the positive-control plasmid pair p53 and pSV40 (Figure 1B, sector 1), the negative-control plasmid pair pLaminC and pSV40 (sector 5), and the plasmid pairs pLaminC and pAD21-1 (sector 2), p53 and pAD21-1 (sector 3), pBD–HHMFP1 and pAD21-1 (sector 4), and pBD–GAL4 and pAD21-1 (sector 6). Only the positive-control pair and the combination of pBD–HHMFP1 and pAD21-1 gave rise to colonies growing on Leu^-, Trp^-, and His^- plates, indicating that no interaction occurs between MAF1 and the GAL4 DNA binding domain or between MAF1 and the unrelated proteins p53 and LaminC. Figure 1C shows a quantification of the β-galactosidase activity of selected strains by *O*-nitrophenyl-β-D-galactopyranoside (ONPG) assays. The combination of pBD–HHMFP1 and pAD21-1 (Figure 1C, bar 3) gave rise to a β-galactosidase activity comparable to that of the positive-control pair p53 and pSV40 (bar 1), whereas the background activities of the combination of pBD–GAL4 with pAD21-1 (bar 4) and of pBD–HHMFP1 with pAD–GAL4 (bar 5) are in the range of the background of the combination of pLaminC and pSV40 (bar 2). Similar results were obtained for pAD6-3 and pAD40-1 (data not shown).

To rule out the possibility that the observed interaction between HHMFP1 and MAF1 was due to newly created features of the respective fusion proteins, we swapped the GAL4 activation and DNA binding domains of the fusion

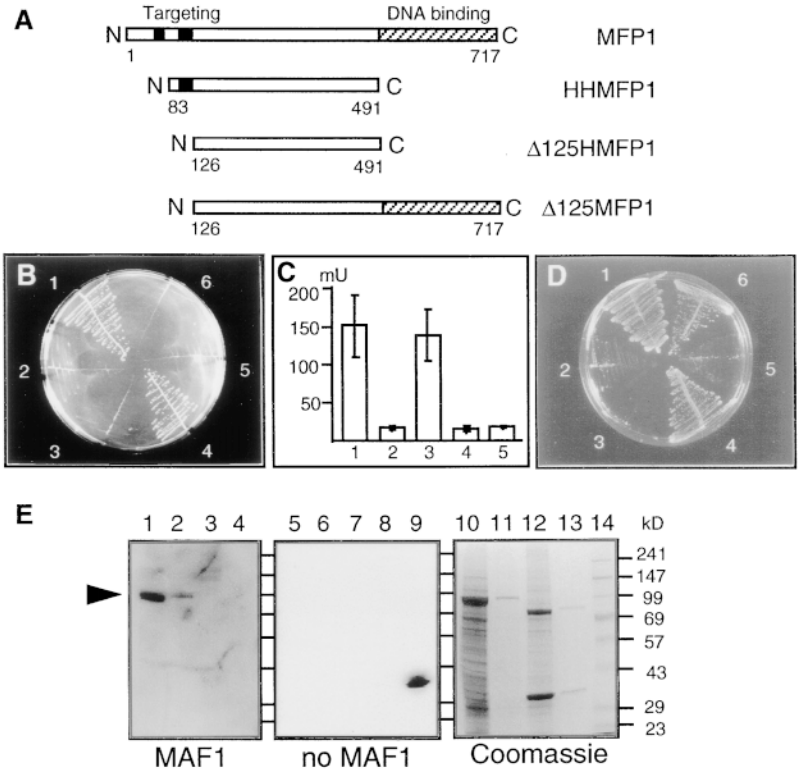

Figure 1. Interaction of MFP1 with MAF1.

(A) Schematic representation of MFP1 indicating the two N-terminal hydrophobic domains as filled bars and the C-terminal DNA binding domain as a hatched bar. The MFP1 subfragments HHMFP1, Δ125HMFP1, and Δ125MFP1 are shown below. Numbers indicate the first and last amino acids of the protein subfragments.

(B) Test for specificity of the pBD–HHMFP1/pAD21-1 interaction. Yeast cells were contransformed with p53 and pSV40 (sector 1), pLaminC and pAD21-1 (sector 2), p53 and pAD21-1 (sector 3), pBD–HHMFP1 and pAD21-1 (sector 4), pLaminC and pSV40 (sector 5), and pBD–GAL4 and pAD21-1 (sector 6); transformants were streaked on Leu^-, Trp^-, and His^- plates.

(C) Quantification of β-galactosidase activity by ONPG assays of yeast strains cotransformed with p53 and pSV40 (bar 1), pLaminC and pSV40 (bar 2), pBD–HHMFP1 and pAD21-1 (bar 3), pBD–GAL4 and pAD21-1 (bar 4), and pBD–HHMFP1 and pAD–GAL4 (bar 5). Mean values and standard deviations of three assays are shown. mU, milliunits.

(D) Confirmation of the MFP1–MAF1 interaction in yeast. Yeast cells were cotransformed with p53 and pSV40 (sector 1), pBD–GAL4 and pAD–HHMFP1 (sector 2), pBD–MAF1 and pAD–GAL4 (sector 3), pBD–MAF1 and pAD–HHMFP1 (sector 4), pBD–Δ125HMFP1 and pAD–GAL4 (sector 5), and pBD–Δ125HMFP1 and pAD6-3 (sector 6); transformants were streaked on Leu^-, Trp^-, and His^- plates.

(E) Confirmation of the MFP1–MAF1 interaction by protein overlay analysis. SDS–polyacrylamide gels (10%) were loaded with 4 μL (lanes 1, 5, and 10) or 4 μL of a 1:10 dilution (lanes 2, 6, and 11) of extract from Bac-Δ125MFP1–infected *Trichoplusia ni* cells. The extract contained ~0.5 μg/mL of Δ125MFP1 protein. As a negative control, adjoining lanes were loaded with 4 μL (lanes 3, 7, and 12) or 4 μL of a 1:10 dilution (lanes 4, 8, and 13) of wild-type baculovirus-infected *Trichoplusia ni* cell extract spiked with 0.5 μg/mL of BSA. After electrophoresis, the gels were stained with Bluprint Fast–PAGE Coomassie stain (lanes 10 to 14) or transferred to a nitrocellulose membrane (lanes 1 to 9). The membrane was divided in half and probed with purified MAF1 protein (lanes 1 to 4) or binding buffer alone (lanes 5 to 9), and immunoblot analysis was subsequently performed with anti-MAF1 antiserum. Lane 9, 15 ng MAF1 protein; lane 14, Benchmark protein ladder (Life Technologies), with molecular masses given in kilodaltons at right. The arrowhead indicates the position of Δ125MFP1.

proteins. Figure 1D shows that the combination of pBD–MAF1 and pAD–HHMFP1 (sector 4), but not pBD–MAF1 and pAD–GAL4 (sector 3) or pBD–GAL4 and pAD–HHMFP1 (sector 2), leads to the specific activation of the *HIS3* gene, indicating that the observed interaction is independent of the orientation in which the yeast two-hybrid assay was performed.

To corroborate the protein–protein interaction observed with the yeast two-hybrid system, we performed a protein overlay experiment with recombinant MFP1 and MAF1. For this experiment, a protein extract from *Trichoplusia ni* cells containing baculovirus-expressed recombinant Δ125MFP1 (Figure 1A) was used. We deleted both hydrophobic domains

of MFP1 to circumvent solubility problems of the overexpressed protein. Figure 1D shows that deletion of the second hydrophobic domain, which is present on HHMFP1, does not affect the observed interaction between MAF1 and MFP1 in the yeast two-hybrid assay, because pBD–Δ125HMFP1 and pAD–MAF1 (sector 6) are capable of activating the *HIS3* gene.

Figure 1E shows the results of the protein overlay experiment. Two different dilutions of a crude protein extract from *Trichoplusia ni* expressing Δ125MFP1 were run alongside the same dilutions of an extract from *Trichoplusia ni* infected with wild-type baculovirus expressing the 29-kD polyhedrin protein. The latter extract was spiked with BSA as an additional negative-control protein with a size comparable to Δ125MFP1 (Figure 1E, lanes 10 to 13). The gel was blotted to nitrocellulose membrane, which was cut in half and incubated either with purified recombinant MAF1 and subsequently an anti-MAF1 antibody (Figure 1E, lanes 1 to 4) or with the anti-MAF1 antibody alone (Figure 1E, lanes 5 to 9). An additional lane contained 15 ng of purified MAF1 as immunoblot control (Figure 1E, lane 9). A replica gel was stained with Bluprint Fast–PAGE Coomassie stain (Figure 1E, lanes 10 to 14). Under these conditions, MAF1 specifically bound to Δ125MFP1, whereas no binding to polyhedrin, BSA, or any other viral or cellular protein was detected (Figure 1E, lanes 1 to 4). In the absence of MAF1, no signal was detected (Figure 1E, lanes 5 to 8). To show that not only MAF1 but also MFP1 binds specifically, the experiment was repeated using ovalbumin rather than MAF1 as a probe, and detection was conducted with an anti-ovalbumin antibody. No signal was detected in this experiment (data not shown). These data show that MAF1 specifically binds to MFP1 in vitro and that the binding not only occurs to HHMFP1 but also to the larger Δ125MFP1, which contains the DNA binding domain.

MAF1 Is a Novel Protein

DNA sequencing of the cDNA inserts of pAD21-1, pAD40-1, and pAD6-3 showed that they code for the same protein. The cDNA insert of pAD6-3 lacks 19 nucleotides at the 5′ end compared with the other two inserts. Apart from this, the three DNA sequences are identical, except for a divergence in the 3′ untranslated regions, in which the pAD21-1 sequence differs from the pAD6-3 and pAD40-1 sequences. All three cDNAs contain an ATG codon in a sequence environment (ACCGATGGC) with good similarity to the consensus sequence for ATG start codons in plants (AACAATGGC; Lutke et al., 1987) that is followed by an open reading frame encoding a protein of 152 amino acids with a predicted molecular mass of 16.2 kD. Figure 2A shows the deduced amino acid sequence of MAF1. MAF1 is a hydrophilic protein with alternating acidic and basic domains and a high percentage of serine and threonine residues (15% serine and 9% threonine; Figure 2B). A BLAST (Altschul et al., 1997) search of the protein databases showed no significant sequence similarity with known proteins, indicating that MAF1 is a novel protein.

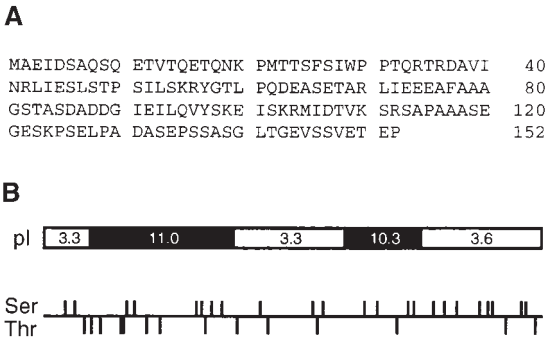

Figure 2. Sequence and Structural Organization of MAF1.

(A) The deduced amino acid sequence of MAF1 is in single-letter code. The GenBank accession number is AF118113.

(B) Structural organization of MFP1. At top is the distribution of acidic and basic domains. Acidic domains are indicated by open bars, and basic domains are indicated by filled bars. Numbers indicate the calculated pI values of the respective domains. At bottom is the distribution of serine and threonine residues. Lines above the horizontal line indicate serine residues; lines below the horizontal line indicate threonine residues.

Genomic Organization and Expression of MAF1

Genomic DNA gel blot analysis indicated that MAF1 is encoded by a single gene in tomato (Figure 3A). A single band was detected with all restriction enzyme combinations, except for BamHI (Figure 3A, lane 4). The two bands detected in the BamHI digest can be accounted for by the single BamHI site in the MAF1 cDNA. These data suggest that *MAF1* is a single-copy gene and that the polymorphism in the 3′ untranslated regions of the three isolated cDNAs is due to allelic variation. The expression of MAF1 was examined in different tissues of tomato by RNA gel blot analysis and immunoblot analysis. Figure 3B shows that the *MAF1* probe detected a single RNA species of ~700 nucleotides in size, which is consistent with the length of the isolated cDNAs. *MAF1* mRNA accumulation was detected in young tomato leaves, young fruits, and flowers, indicating that *MAF1* is expressed in different plant tissues. The anti-MAF1 antibody detected a single protein of ~25 kD in young fruits, young leaves, flowers, and stems (Figure 3C), which is consistent with the abundance of the *MAF1* RNA. The size of the protein, as determined by SDS-PAGE, is somewhat larger than is the predicted molecular mass of 16.2 kD. This is most likely due to abnormal migration of the protein, because the recombinant protein expressed in *Escherichia coli* shows the same discrepancy between predicted and observed size (Figure 1E, lane 9 and data not shown). Figure

3D shows an immunoblot comparing leaf protein extracts from tomato and tobacco. The anti-MAF1 antibody detected a single band in tobacco that is of slightly smaller size than is tomato MAF1, indicating that a closely related homolog of MAF1 is present in tobacco. No bands were detected with the preimmune serum in either tomato or tobacco under identical conditions (data not shown).

MAF1 Is Located at the Nuclear Envelope

A way to prove the in vivo interaction of soluble proteins is to perform a coimmunoprecipitation experiment with a plant protein extract. In our case, this experiment was not possible, because only a marginal amount of MFP1 is present in a soluble protein extract (data not shown). The majority of MFP1 is insoluble, most likely due to its localization at the nuclear envelope and attachment to the nuclear matrix (Gindullis and Meier, 1999). In addition, most of the MAF1 in plant protein extracts appears to be insoluble as well (data not shown).

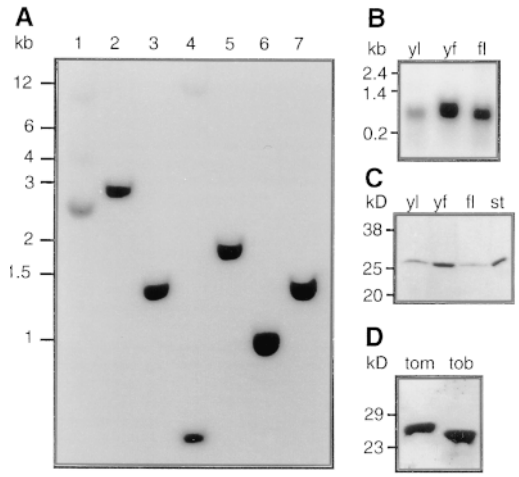

Figure 3. Genomic Organization and Expression of MAF1.

(A) Genomic DNA gel blot analysis. Tomato genomic DNA was digested with EcoRI (lane 1), HindIII (lane 2), EcoRV (lane 3), BamHI (lane 4), EcoRI and HindIII (lane 5), EcoRI and EcoRV (lane 6), and EcoRV and HindIII (lane 7). DNA length markers are indicated at left in kilobases. The 12-kb BamHI signal has reduced intensity due to partial transfer of high molecular weight DNA. The faint bands in the EcoRI digest (lane 1) are most likely due to incomplete digestion, because no additional bands were detected in the EcoRI and HindII and the EcoRI and EcoRV double digests (lanes 5 and 6).

(B) RNA gel blot analysis with total RNA isolated from different tomato tissues. RNA length markers are indicated at left in kilobases. Equal amounts of total RNA were loaded in each lane, as determined by ethidium bromide staining of the rRNAs. yl, young leaf; yf, young fruit; fl, flower.

(C) Immunoblot analysis with total protein extracts from different tomato tissues. Protein mass markers are indicated at left in kilodaltons. Equal amounts of protein were loaded in each lane as determined by staining with Bluprint Fast–PAGE stain of a replica gel. yl, young leaf; yf, young fruit; fl, flower; st, stem.

(D) Immunoblot analysis of leaf extracts from tomato (tom) and tobacco (tob). Equal amounts of protein were loaded in both lanes as determined by staining with Bluprint Fast–PAGE stain of a replica gel. Molecular mass markers are indicated at left in kilodaltons.

As an alternative approach to investigate whether MFP1 and MAF1 are potential interaction partners in the plant cell, we compared the subcellular localization of MAF1, as determined by transient transformation of an MAF1–green fluorescent protein (GFP) fusion protein, with that of MFP1. We have shown previously that MFP1 is located in specklelike structures at the nuclear envelope (Gindullis and Meier, 1999). Because a fusion of MAF1 and mutant GFP (mGFP) would have a molecular mass of only 43 kD, it might be able to diffuse passively into the nucleus (Grebenok et al., 1997). Therefore, the sandwich fusion MAF1–mGFP–MAF1, which has a molecular mass of 59 kD, was expressed (Figure 4A). This fusion protein should enter the nucleus only if a nuclear localization signal is present on MAF1. Figures 4B and 4C show an NT-1 cell that was transiently expressing MAF1–mGFP–MAF1 after particle bombardment. GFP fluorescence clearly accumulated at the nuclear envelope, where it appeared to be evenly distributed. In addition, a weaker signal was detected in the cytoplasm and inside the nucleus, excluding the nucleolus. The cytoplasmic fluorescence pattern appeared uneven, and tracklike and specklelike signals were observed. Figures 4D and 4E show a control transformation with mGFP. As expected, mGFP accumulated evenly in the cytoplasm as well as the nucleus, with no specific pattern of accumulation. To verify the localization pattern observed with the GFP protein fusions, MAF1 was also localized in fixed NT-1 cells by immunocytochemistry. Figures 5A to 5C show that the anti-MAF1 antibody decorated predominantly the nuclear periphery, with some weaker signal present in the cytoplasm and the nucleus. No signal was detected under identical conditions when the preimmune serum was used (data not shown). Together, these data show that MAF1 is predominantly located at the nuclear periphery. Its sharp, ringlike distribution pattern is consistent with a location in or close to the nuclear envelope.

MAF1 Is Associated with the Nuclear Matrix

We have shown that MFP1 is located at specklelike structures at the nuclear periphery and that these structures are a part of isolated nuclei and of the nuclear matrix (Gindullis and Meier, 1999). The localization of MAF1 at the nuclear periphery together with the yeast two-hybrid and in vitro binding data suggest that MFP1 and MAF1 interact in vivo. To confirm this correlation further, we investigated whether MAF1 is, like MFP1, a component of isolated nuclei and of the nuclear matrix. Figures 5D and 5E show that MAF1 was detected at the rim of isolated nuclei, indicating that it is

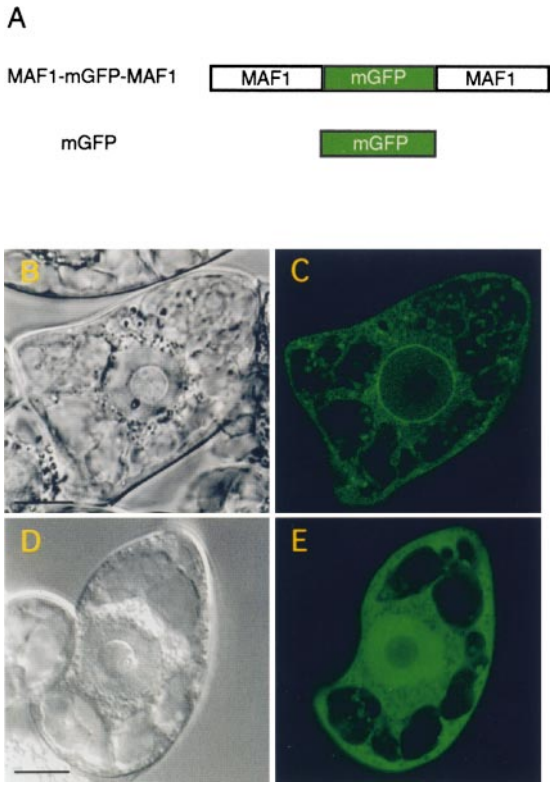

Figure 4. Localization of MAF1–mGFP–MAF1 Fusion Protein in Tobacco NT-1 Cells.

(A) Schematic representation of the proteins transiently expressed in tobacco NT-1 cells.
(B) Differential interference contrast image of the cell shown in **(C)**.
(C) GFP fluorescence of a cell transiently expressing MAF1–mGFP–MAF1 after particle bombardment–mediated transformation.
(D) Differential interference contrast image of the cell shown in **(E)**.
(E) GFP fluorescence of a cell transiently expressing mGFP after particle bombardment–mediated transformation.

Bars in **(B)** and **(D)** = 10 μm for **(B)** to **(E)**.

tightly associated with the nucleus, even after treatment with Triton X-100, which should remove most of the outer membrane of the nuclear envelope (Watson and Thompson, 1986). Figures 5F and 5G show that immunoreactive material was still visible in a nuclear matrix fraction. In contrast to the staining pattern seen in intact nuclei, MAF1 was no longer located at the rim but concentrated around the nucleolus (cf. Figures 5F and 5G). This is consistent with a collapse of the structures containing MAF1, very similar to what has been shown for the redistribution of MFP1 after nuclear matrix preparation (Gindullis and Meier, 1999). These data show that MFP1 and MAF1 have an overlapping localization pattern at the nuclear periphery and that both proteins behave identically during isolation of the nuclear matrix, strongly suggesting that they are components of the same or of tightly connected nuclear structures.

MAF1 Is Conserved among Higher Plants

Whereas MAF1 is a novel protein with no significant similarity to other proteins in the databases, the sequence of a recently submitted Arabidopsis bacterial artificial chromosome clone (GenBank accession number AB008267) from chromosome 5 contains an MAF1-related open reading frame. In addition, a number of expressed sequence tags (ESTs) from different higher plant species were found to contain open reading frames with significant sequence similarity to MAF1. The alignment of these protein sequences is shown in Figure 6A. The sequences from tomato, Arabidopsis, soybean, and maize contain the full MAF1 open reading frame, whereas the *Canna edulis*, *Picramnia pentandra*, and wheat sequences represent only the N-terminal portion of these proteins. The most pronounced sequence similarity is found in the central part of the proteins, with two blocks of highly conserved sequence separated by a less conserved stretch of ~30 amino acids. The N and C termini of the aligned proteins show significantly less sequence similarity. Figure 6B shows a comparison of the most highly conserved sequence blocks with the charge profile of tomato MAF1. The sequence conservation roughly coincides with the two basic domains of the protein. The most highly conserved motif is the sequence IWPPTQRTRDAV in the first basic domain, which is nearly 100% conserved between seven sequences, with the only two mismatches being conservative ex-

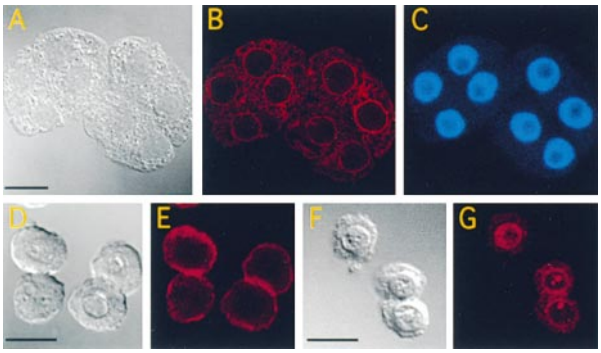

Figure 5. Immunolocalization of MAF1 in NT-1 Cells, NT-1 Nuclei, and the NT-1 Nuclear Matrix.

(A), **(D)**, and **(F)** Differential interference contrast images of fixed NT-1 cells **(A)**, NT-1 nuclei **(D)**, and an NT-1 nuclear matrix fraction **(F)**.
(B), **(E)**, and **(G)** Detection of MAF1 with the anti-MAF1 antibody R37 and a Cy5-conjugated goat anti–rabbit secondary antibody in NT-1 cells **(B)**, NT-1 nuclei **(E)**, and an NT-1 nuclear matrix fraction **(G)**.
(C) 4′,6-Diamidino-2-phenylindole (DAPI) staining of the nuclei of the NT-1 cells shown in **(A)** and **(B)**.
Bar in **(A)** = 20 μm; bars in **(D)** and **(F)** = 10 μm.

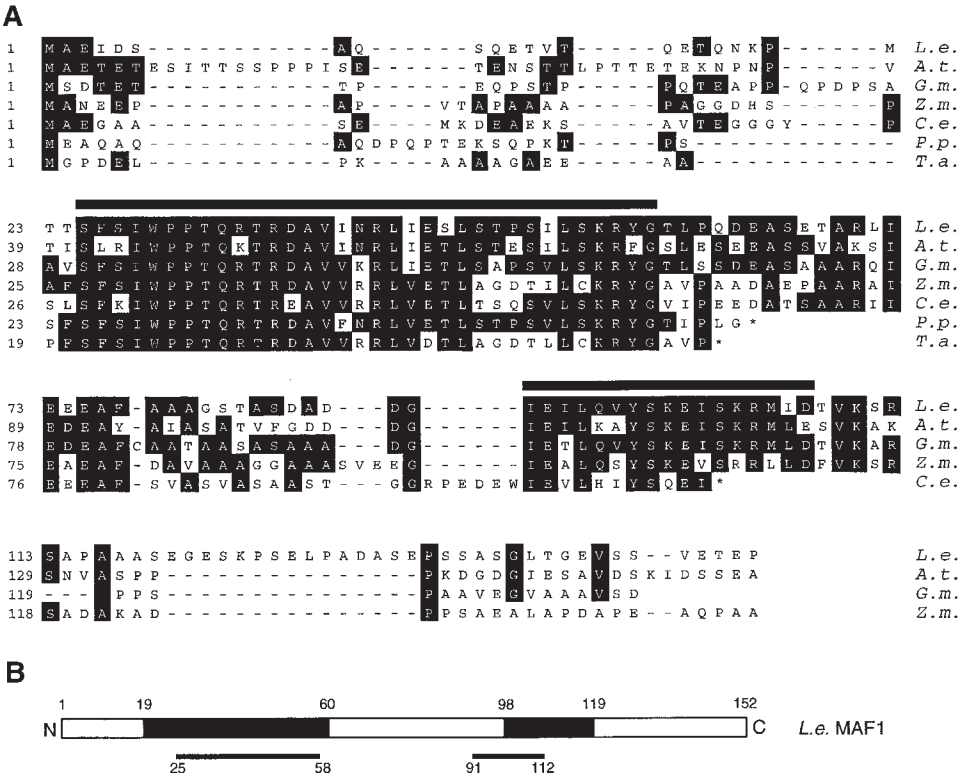

Figure 6. MAF1 Is Conserved among Higher Plants.

(A) Alignment of deduced protein sequences of full-length cDNAs and ESTs from different plant species. Identical amino acids are shown by reverse lettering. The two most highly conserved domains are indicated by black bars above the sequence. Dashes indicate gaps in the alignment. Numbers at left refer to amino acid position in each sequence. Asterisks indicate the ends of the ESTs. *L.e.*, *Lycopersicon esculentum*; *A.t.*, *Arabidopsis thaliana*; *G.m.*, *Glycine max*; *Z.m.*, *Zea mays*; *C.e.*, *Canna edulis*; *P.p.*, *Picramnia pentandra*; *T.a.*, *Triticum aestivum.* The GenBank accession numbers are AF118113, AB008267, AF118115, AF118114, AF118116, AF118117, and AF118118, respectively.
(B) Comparison of the positions of the most highly conserved sequences (black lines) and the basic domains (filled bars) in tomato MAF1. Numbers indicate amino acid positions. *L.e.*, *Lycopersicon esculentum.*

changes of charged amino acids. No other proteins containing this sequence motif have been found in the databases.

DISCUSSION

MAF1 Is a Novel Protein That Is Well Conserved among Higher Plants

In this report, we describe the cloning and characterization of a novel protein, MAF1, that interacts with the plant MAR binding protein MFP1. MAF1 is a small, serine/threonine-rich protein that has no similarity to previously described proteins but has now been found to be well conserved among higher plants. MAF1 homologs have been identified in seven plant species, including both dicots and monocots (Figure 6). Whereas the N- and C-terminal parts of the proteins have little sequence similarity, the central part, and in particular the two basic domains, are well conserved. Most striking is a 12–amino acid motif that is nearly 100% identical between the seven sequences, with the only two exchanges being conservative replacements of charged amino acids. Because this motif is not present in any other proteins in the databases, it might represent a signature sequence for MAF1-like proteins and is a good candidate for a functional domain.

MAF1 Is Located at the Nuclear Envelope but Is Not a Membrane-Attached Protein

Both immunolocalization and GFP localization experiments indicate that MAF1, similar to MFP1, is located at the nuclear envelope. In addition, a fraction of the protein is located in the cytoplasm, in a fibrillar pattern resembling the

appearance of endoplasmic reticulum (ER) in tobacco cells (Restrepo-Hartwig and Ahlquist, 1996; Schaad et al., 1997). The localization pattern of MAF1 is similar to the one described for the animal lamin B receptor (LBR), an integral membrane protein of the inner nuclear membrane (Ellenberg et al., 1997). In transient LBR–GFP localization experiments, GFP fluorescence was detected at early stages after transformation in the cytoplasm, colocalizing with ER markers, whereas it accumulated at later stages at the nuclear periphery, with a constant low steady state signal in the ER (Ellenberg et al., 1997). This pattern has been interpreted as a synthesis of LBR at ER membranes, followed by a transport to the nuclear envelope.

In contrast to the eight membrane-spanning domains found in LBR, MAF1 does not appear to contain any membrane attachment regions. It contains neither hydrophobic domains nor a C-terminal farnesylation sequence (Schafer and Rine, 1992). In addition, there is no indication for an N-terminal signal peptide (Nielsen et al., 1997) or for an ER retention sequence that would indicate that MAF1 is translated at the rough ER. Therefore, it is likely that the association of MAF1 with the nuclear envelope and with the cytoplasmic structures is not due to direct membrane attachment. This assumption is also consistent with the finding that MAF1, like MFP1, is located on the rim of isolated nuclei, which should be stripped at least of the outer nuclear membrane (Watson and Thompson, 1986), and with the observation that MAF1 is present in a nuclear matrix preparation that should be free of any membrane material (Verheijnen et al., 1988).

If MAF1 is not a membrane-attached protein, its localization at the nuclear envelope and the resemblance of its cytoplasmic localization pattern with ER might be caused by a connection with the plant cytoskeleton. A close connection between the membrane systems and actin filaments recently has been shown in plants (Boevink et al., 1998). It is interesting in this context that plant importin α, a component of the nuclear localization signal receptor, has been found associated with both actin and tubulin in the cytoplasm (Smith and Raikhel, 1998). Hence, a connection might exist between functional proteins of the nuclear envelope and elements of the cytoplasmic cytoskeleton. Colocalization experiments with MAF1 and actin and tubulin will allow further characterization of the cytoplasmic localization of MAF1.

Localization Patterns of MFP1 and MAF1 Overlap at the Nuclear Envelope

The localization patterns of MAF1 and MFP1 overlap at specific sites of the nuclear envelope, suggesting that the two proteins interact in vivo. MFP1 is most likely attached to membranes via its N-terminal hydrophobic domains (Gindullis and Meier, 1999) and therefore could provide anchoring to the nuclear envelope for a soluble protein such as MAF1. However, the difference between the specklelike localization of MFP1 and the continuous localization of MAF1 suggests that MAF1 must be attached to the nuclear envelope by additional means. One formal possibility is the formation of MAF1 homooligomers that are attached to the nuclear envelope by interacting with MFP1 at the specklelike structures. Because MAF1 runs as a monomer in native protein gels and does not dimerize in the yeast two-hybrid screen (data not shown), this scenario is rather unlikely. Hence, MAF1 is likely in contact with additional, unidentified proteins of the plant nuclear periphery. Interestingly, MAF1 interacts, in a yeast two-hybrid screen, with four additional, novel, coiled-coil–like proteins from tomato (F. Gindullis and I. Meier, unpublished results). Although the subcellular localization of these proteins has not been determined, it is conceivable that MAF1 is a molecule that connects different coiled-coil filament proteins involved in forming a nucleoskeletal layer at the nuclear envelope and that one spatially specific interaction is the one with MFP1. Interestingly, another coiled-coil–like protein, designated NMCP1, which has been reported recently from carrot, is located at the nuclear periphery in a pattern very similar to that of MAF1 (Masuda et al., 1997). It will be worthwhile to test whether MAF1, as well as MFP1 and the new MAF1 binding proteins, can interact with NMCP1.

MAF1 and MFP1 Are Connected to a Subcomponent of the Plant Nuclear Matrix

The fact that both MAF1 and MFP1 remain on the rim of isolated nuclei and collapse into the interior of the nuclear matrix strongly suggests that they are parts of the same macromolecular complex. The collapse of nuclear periphery material is not a general phenomenon or an artifact of the nuclear matrix preparation. The plant antigen of the monoclonal antibody mAb6C6, which was raised against animal centrosomal material (Chevrier et al., 1992), also is located at the rim of isolated tobacco NT-1 nuclei (Gindullis and Meier, 1999). In contrast to MFP1 and MAF1, it remains in specklelike structures at the rim of the nuclear matrix, indicating that the corresponding relocalization of MFP1 and MAF1 is significant and that the mAb6C6 antigen is most likely a component of a different structure (Chevrier et al., 1992; Gindullis and Meier, 1999).

The most likely explanation for the association of MFP1 and MAF1 with isolated nuclei and the nuclear matrix is that they are attached to additional proteins that form a rigid structure lining the nuclear envelope. Upon nuclear matrix preparation, this structure collapses from the nuclear periphery toward the nuclear interior but stays connected with the material representing the nuclear matrix. This is consistent with the existence of a specific proteinaceous component of the nuclear skeleton located at the nuclear periphery. Interestingly, a very similar behavior has been described for the animal nuclear pore–lamina complex (Verheijnen et al., 1988). The lamina and the nuclear pores

are tightly connected in animal cells and appear as part of the nuclear matrix after the removal of the nuclear envelope membranes. This indicates the presence of a tightly linked nuclear suprastructure that includes nuclear pores, the lamina, and the filaments of the internal nuclear matrix. The specific localization of MFP1 and MAF1 together with their conjoint behavior during nuclear matrix preparation now suggest the presence of a structurally similar, although probably molecularly different, complex in plants.

METHODS

Plant Material

Tomato (*Lycopersicon esculentum* cv VFNT cherry) and tobacco (*Nicotiana tabacum*) plants were grown under greenhouse conditions. Tobacco suspension-cultured cells (NT-1 cells) were cultured as described previously (Allen et al., 1996). For all experiments, aliquots from a mid-log phase culture (day 5 to 6) were used.

Construction and Screening of a Yeast Two-Hybrid Library

Total RNA from young tomato leaves was isolated as described by Wanner and Gruissem (1991), and mRNA was purified using an mRNA purification kit (Pharmacia Biotech, Piscataway, NJ). The yeast two-hybrid library was constructed using the cDNA synthesis kit, the Gigapack III gold packaging extract, and the HybriZAP two-hybrid predigested vector kit (all from Stratagene), according to the protocol of the manufacturer. The size of the primary library was determined to be 1.5×10^6 plaque-forming units. All steps of the library screening, including the transformation, the isolation of clones, and the verification of the interactions, were performed as described by the manufacturer.

Plasmid Vectors

The 1227-bp HincII fragment of pRSETA–MFP1 (Meier et al., 1996) containing the central, α-helical part of MFP1 (Figure 1A) was cloned into pBD–GAL4 (Stratagene) by using the filled-in EcoRI site to create pBD–HHMFP1. The plasmids pAD6-3, pAD21-1, and pAD40-1 contain the complete MAF1 open reading frame and were isolated from a tomato leaf library in a yeast two-hybrid screen, using pBD–HHMFP1 as a bait construct. The plasmid p11-3 contains the complete MAF1 open reading frame and was obtained by screening a λ ZAP library of young tomato fruits (Meier et al., 1996), using the cDNA insert of pAD6-3 as a probe. For confirmation of the MFP1–MAF1 interaction, the cDNA insert of pAD6-3 was cloned as an EcoRI-XhoI fragment into the EcoRI and SalI sites of the yeast two-hybrid bait vector pBD–GAL4 to create pBD–MAF1. The 1227-bp HincII fragment of MFP1 (Figure 1A) was cloned into the filled-in EcoRI site of the prey vector pAD–GAL4 (Stratagene) to create pAD–HHMFP1. The vector pBD–Δ125HMFP1, which lacks both transmembrane domains of MFP1 (Figure 1A), was created by cloning the filled-in NcoI-HincII fragment from pMFP1–Δ125–mGFP (Gindullis and Meier, 1999) into the filled-in EcoRI site of pBD–GAL4. All constructs were confirmed by sequencing.

To express the MFP1 protein in insect cells by use of the baculovirus expression system, we cloned an NcoI fragment from pMFPΔ125–mGFP containing amino acids 126 to 717 into the NcoI site of the vector pFastBac HTc (Life Technologies, Gaithersburg, MD) to create pFastBac–Δ125MFP. The vector pmGFP–MAF1 was constructed by inserting the filled-in EcoRI-XhoI fragment of p11-3 into the single, filled-in BglII site of pRTL2–mGFPS65T (von Arnim et al., 1998). To create pMAF1–mGFP–MAF1, the open reading frame of MAF1 was amplified by polymerase chain reaction (PCR) using the primers 5′-CACCCATGGCGGAAATCG-3′ and 5′-TACCTCCCATGGGCTCGG-3′ and p11-3 as a template. The resulting PCR product was cloned into the single NcoI site of pmGFP–MAF1 using the internal NcoI sites of the PCR primers. The correct sequence of the PCR product was confirmed by sequencing. The cDNA insert of pAD6-3 was cloned as an EcoRI-XhoI fragment into the EcoRI and XhoI sites of pBluescript SK II+ (Stratagene) to create pBS6-3. The PstI-PstI and PstI-KpnI fragments of pBS6-3 were gel purified and ligated in a three-way ligation into the PstI and KpnI sites of pRSETC (Invitrogen, Carlsbad, CA) to create pRSETC– MAF1.

The plasmid vectors p53, pLaminC, and pSV40 are components of the HybriZAP Two-Hybrid Predigested Vector Kit (Stratagene). p53 expresses a fusion protein of the GAL4 DNA binding domain and the amino acids 72 to 390 of murine p53 (Iwabuchi et al., 1993); pLaminC expresses a fusion protein of the GAL4 DNA binding domain and the amino acids 67 to 230 of human lamin C (Bartel et al., 1993); and pSV40 expresses a fusion protein of the GAL4 activation domain and the amino acids 84 to 708 of the SV40 large T-antigen (Chien et al., 1991).

O-Nitrophenyl-β-D-Galactopyranoside Assay

The yeast reporter strain YRG-2 (Stratagene) was cotransformed with the indicated plasmid vectors, plated on selection medium (synthetic complete medium lacking leucine and tryptophan for selection of cotransformants), and incubated for 3 to 4 days at 30°C according to the protocol of the manufacturer. By using single colonies (~2 mm in diameter), 10 mL of overnight cultures with selection medium were inoculated and grown at 30°C with vigorous shaking (300 rpm). After ~16 hr, fresh YPD medium (20 g/L peptone [BDMS/Difco Laboratories, Franklin Lakes, NJ], 10 g/L yeast extract [BDMS/Difco Laboratories], and 2% glucose, pH 5.8) was inoculated with the overnight cultures at an $OD_{600\ nm}$ of 0.2 and grown as above to an $OD_{600\ nm}$ of 0.4 to 0.7. Ten milliliters of the cultures was centrifuged at 4000*g* for 10 min at room temperature and resuspended in 0.5 mL of Z buffer (16.1 g/L $Na_2HPO_4 \times 7H_2O$, 5.5 g/L $NaH_2PO_4 \times 7H_2O$, 0.75 g/L KCl, 0.246 g/L $MgSO_4$, and 2.7 mL/L β-mercaptoethanol). Cells were broken by adding 300 μL of acid-washed glass beads (Sigma) and vortexing three times for 3 min. Samples were cooled on ice for 1 min after each vortexing step. To clear the extracts, samples were centrifuged for 10 min at 4°C and 15,000 rpm in a tabletop centrifuge. The cleared supernatants were transferred to fresh tubes and stored on ice. To the pelleted cell debris, 0.5 mL of Z buffer was added, and the samples were vortexed for another 3 min. Samples were cleared as above, and supernatants were combined. To 750 μL of each supernatant, 160 μL of *O*-nitrophenyl-β-D-galactopyranoside (ONPG) solution (4 mg/mL ONPG in 0.1 M sodium phosphate buffer, pH 7.0) was added, and reactions were incubated at 30°C until a yellow color developed (2 to 100 min). To stop the reactions, 400 μL of 1 M Na_2CO_3 was added, and the $OD_{420\ nm}$ was determined photometrically. Units of β-galactosidase were calculated using the following equation:

$$\text{activity (units)} = \text{OD}_{420\ \text{nm}} \times 1000 / (\text{OD}_{600\ \text{nm}} \times V \times t),$$

where t is the time of incubation in min, V is the used culture volume in milliliters, and $\text{OD}_{600\ \text{nm}}$ is the optical density at 600 nm of the culture used in the assay.

MAF1 Charge Profile Analysis

Charge profile analysis of MAF1 was performed using the protein analysis program and the sequence editing and analysis program of the DNASTAR package (DNASTAR Inc., Madison, WI).

MAF1 Protein Expression and Purification and Antibody Production

To express the recombinant MAF1 protein with an N-terminal histidine tag, *Escherichia coli* BL21 cells (Novagen, Madison, WI) were transformed with pRSETC–MAF1, and expression was induced by isopropyl-β-D-thiogalactoside, according to the Qiagen protein expression manual (Qiagen, Chatsworth, CA). Recombinant MAF1 was purified by nickel-affinity chromatography, as described in the Qiagen protein expression manual. For immunization of New Zealand white elite rabbits, nickel-affinity chromatography was followed by SDS-PAGE. The band corresponding to the MAF1 fusion protein was excised from the gel, and the gel slice was air dried. Antisera were produced by Covance Research Products (Denver, PA), using the company's standard immunization protocol.

Expression of Δ125MFP1 in Insect Cells by Using the Baculovirus Expression System

Recombinant baculovirus encoding MFP1Δ125 (Figure 1A), designated Bac-Δ125MFP1, was prepared as described in the BAC-TO-BAC Expression System Manual (Life Technologies), using the vector pFastBac–MFPΔ125. *Trichoplusia ni* (BTI-Tn-5B1-4) cells (Granado et al., 1994) were infected at a multiplicity of infection of 5 to 10 and grown in ExCell 405 media (JRH Biosciences, Lenexa, KS) for production of protein and yielded ~100 μg of Δ125MFP1 protein per 10^6 cells (Figure 1E, lane 10). Cells infected with wild-type baculovirus were grown under similar conditions.

Protein Overlay Analysis of the MFP1–MAF1 Interaction

Trichoplusia ni cells (10^6 cells) infected with Bac-Δ125MFP1 or wild-type baculovirus were lysed in 200 μL of Laemmli sample buffer (Bio-Rad). The wild-type extract was spiked with 100 μg of BSA (Sigma) to provide a second control protein of similar size and concentration to Δ125MFP1 in addition to the 29-kD polyhedrin protein. The protein extracts (4 μL, or 4 μL of a 1:10 dilution) were separated on 10% polyacrylamide gels and blotted to a nitrocellulose membrane in Tris-glycine buffer containing 20% methanol and 0.05% SDS, according to the manufacturer (Bio-Rad). After a brief rinse in binding buffer (20 mM Hepes, 40 mM NaCl, 0.1 mM EDTA, 0.5 mM dithiothreitol, and 5% glycerol, pH 7.8), the proteins were denatured by incubating for 45 min in binding buffer containing 6 M guanidine HCl and then slowly renatured by incubating in binding buffer with 3, 1.5, 0.75, and 0.375 M guanidine HCl for 15 min each. After a 15-min wash in binding buffer, the blots were blocked for 3 hr in binding buffer plus 5% nonfat dry milk, followed by three washes in binding buffer for a total of 10 min. The membranes were incubated overnight with 50 μg/mL purified MAF1 protein in a total volume of 3 mL of binding buffer or with binding buffer alone. After the overnight incubation, the membranes were rinsed once in binding buffer, followed by three rinses in TBST (Sambrook et al., 1989) for a total of 15 min. Bound MAF1 protein was detected by immunoblot analysis with a 1:1500 dilution of the anti-MAF1 antisera R37 and a 1:1500 dilution of horseradish peroxidase–coupled donkey anti–rabbit secondary antibody (Amersham Pharmacia Biotech, Piscataway, NJ) in TBST. The antibody incubations were performed for 20 min each, and the blots were washed for 5 min with three changes of TBST after each incubation. Enhanced chemiluminescent (ECL) detection was performed as described in the ECL manual (Amersham Pharmacia Biotech). All incubations after the transfer were performed at 4°C. A replica filter was probed with 50 μg/mL purified ovalbumin (Sigma) and bound protein detected with anti-ovalbumin antisera (Sigma) under identical conditions to the blot probed with MAF1.

Isolation of Tomato and Tobacco Total Protein Extracts

Fresh tissue (100 mg) was ground in liquid nitrogen to a fine powder. After adding 0.5 mL of extraction buffer (62.5 mM Tris-HCl, pH 6.8, 20% glycerol, 4% SDS, and 1.4 M β-mercaptoethanol), the sample was vortexed for 30 to 60 sec and incubated for 10 min at 70°C. Debris was removed by centrifugation for 10 min at 4°C and 15,000 rpm in a tabletop centrifuge. The cleared supernatant was transferred to a fresh tube and stored at −80°C. Aliquots were boiled for 5 min before SDS-PAGE.

Immunoblot Analysis

A 1:3000 dilution of the anti-MAF1 antisera R37 or R38 and a 1:10,000 dilution of horseradish peroxidase–coupled donkey anti–rabbit secondary antibody (Amersham Pharmacia Biotech) were used to perform immunoblot analysis as described by Sambrook et al. (1989). ECL detection was performed as described by the manufacturer (Amersham Pharmacia Biotech). Protein gels were stained with Bluprint Fast–PAGE Coomassie stain (Life Technologies).

RNA Gel Blot Analysis

Total RNA from tomato leaves (5 to 15 mm), fruits (3 to 8 mm in diameter), and whole flowers was isolated with the Trizol Reagent from Life Technologies. Total RNA (10 μg each) was separated on a formaldehyde gel, blotted to a nitrocellulose membrane, and hybridized with the radioactively labeled 533-bp EcoRI-PstI fragment of the 6-3 cDNA essentially as described by Sambrook et al. (1989). Signals were detected after a 3-day exposure of x-ray film to the blot using an intensifying screen.

Genomic DNA Gel Blot Analysis

Genomic DNA from tomato was isolated as described by Dellaporta et al. (1983). Forty micrograms of genomic DNA was digested with 5 units of the restriction endonucleases indicated in Figure 3 for 3 hr at 37°C. DNA fragments were separated on a 1% agarose gel, blotted onto a nitrocellulose membrane, and hybridized at 65°C for 12 hr with

the radioactively labeled 533-bp EcoRI-PstI fragment of the 6-3 cDNA in 7% SDS, 0.5 M sodium phosphate buffer, pH 7.0, and 1 mM EDTA with 20 μg/mL denatured herring sperm DNA (Life Technologies). Filters were washed (15 min each) in 2 × SSC (1 × SSC is 0.15 M NaCl and 0.015 M sodium citrate), 0.1% SDS at room temperature, 2 × SSC, 0.1% SDS at 65°C, and three times in 0.2 × SSC, 0.1% SDS at 65°C. Signals were detectable after a 20-hr exposure of x-ray film to the blot using an intensifying screen.

Immunolabeling of NT-1 Cells, Nuclei, and Nuclear Matrices

Cells (0.5 mL) of a 3- to 4-day-old NT-1 suspension culture were pelleted in a picofuge (Stratagene) for 15 sec. All of the fixation, permeabilization, labeling, and washing steps were performed in a batch procedure in 1.5-mL tubes, and the cells were pelleted between buffer changes as described above. Cells were fixed in 400 μL of 2% paraformaldehyde in PHEM (60 mM Pipes, 25 mM Hepes, 10 mM EGTA, and 2 mM $MgCl_2$, pH 6.9) and permeabilized in 400 μL of 0.5% (v/v) Nonidet P-40 (Sigma) in PHEM. After washing the cells in 1 mL PBS (7.4 mM Na_2HPO_4, 1.4 mM NaH_2PO_4, and 150 mM NaCl), the samples were blocked overnight in 1 mL of 5% normal goat serum (Molecular Probes, Eugene, OR) and 2% BSA (Sigma) in PHEM. Samples were then incubated for 1 hr at room temperature in the primary antibody, which was diluted 1:70 in blocking solution. Samples were rinsed with 1 mL of PBS, PBS with 0.1% (v/v) Nonidet P-40, and PBS for 5 min each and incubated for 1 hr in a 1:100 dilution of the appropriate Cy5-conjugated secondary antibody (Jackson ImmunoResearch Laboratories Inc., West Grove, PA). Samples were rinsed as before, and aliquots were mounted in Slow Fade (Molecular Probes) with 50% glycerol. Nuclei and nuclear matrices of NT-1 cells were prepared as described by Hall et al. (1991). Indirect immunfluorescence microscopy of nuclei and nuclear matrices was performed as described by Gindullis and Meier (1999).

Ballistic Transformation of NT-1 Cells

Ballistic transformation of NT-1 cells was performed essentially as described by Allen et al. (1996). Approximately one microgram of supercoiled plasmid DNA was used per bombardment. After bombardment, the Petri dishes were sealed with parafilm and incubated overnight at 27°C. The bombarded cells were removed from the plates by resuspending them in 1 mL of NT-1 culture medium, and they were analyzed for GFP expression.

Fluorescence Microscopy

Digitized confocal images of samples were acquired at either 512 × 512 or 1024 × 1024 pixel resolution with a ×100 oil objective (numerical aperture 1.4) on a Zeiss 410 confocal laser scanning microscope (Carl Zeiss Inc., Thornwood, NY), using the 488-nm excitation line of an Omnichrome Ar-Kr laser for GFP, the 633-nm excitation line of the internal He-Ne laser for Cy5, or the 364-nm excitation lines of a Coherent Enterprise UV Ar laser for 4′,6-diamidino-2-phenylindole (DAPI) and appropriate emission filters (495- to 515-nm bandpass for GFP, 670- to 810-nm bandpass for Cy5, and 400- to 435-nm bandpass for DAPI). For differential interference contrast images, the excitation lines 488 or 586 nm were used. All plates were assembled electronically with Adobe Photoshop software (Adobe Systems Inc., Mountain View, CA).

Identification of Sequences with Similarity to MAF1

The public *Arabidopsis thaliana* database was searched with the cDNA insert of pAD6-3, using the TBLASTX algorithm. The search revealed an open reading frame on chromosome 5 (P1 clone: MMG4; GenBank accession number AB008267) with 44% identity and 61% similarity on protein level to tomato MAF1.

To identify expressed sequence tags (ESTs) from other organisms, the EST database of E.I. Du Pont de Nemours and Company (Wilmington, DE) was used. cDNA libraries representing mRNAs from various plant tissues were prepared in Uni-ZAP XR vectors according to the manufacturer's protocol (Stratagene). Conversion of the Uni-ZAP XR libraries into plasmid libraries was accomplished according to the protocol provided by Stratagene. Upon conversion, cDNA inserts were contained in the plasmid vector pBluescript SK+. cDNA inserts from randomly picked bacterial colonies containing recombinant pBluescript SK+ plasmids were amplified via PCR using primers specific for vector sequences flanking the inserted cDNA sequences, or plasmid DNA was prepared from cultured bacterial cells. Amplified insert DNAs or plasmid DNAs were sequenced in dye-primer sequencing reactions to generate partial cDNA sequences (ESTs; Adams et al., 1991). The resulting ESTs were analyzed using a fluorescent sequencer (model 377; Perkin-Elmer, Norwalk, CT) .

Plant ESTs with similarity to tomato MAF1 were identified by conducting BLAST (Altschul et al., 1997) searches for similarity to sequences contained in the libraries. Percentage of identity was determined by the method of DNASTAR protein alignment protocol using the Jotun-Hein algorithm (Hein, 1990). Default parameters used for the Jotun–Hein method for multiple alignments included a gap penalty of 11 and a gap-length penalty of 3. The EST DNA sequences were translated in all six reading frames and compared with the amino acid sequences of the tomato MAF1 cDNAs. ESTs scoring >40% similarity of amino acid sequence were considered similar to tomato cDNAs. Full-insert sequences were obtained for selected ESTs. The alignment in Figure 6 was done in Megalign (part of the DNASTAR package), using the CLUSTAL algorithm with the default parameters of a gap penalty of 10 and a gap-length penalty of 10.

ACKNOWLEDGMENTS

We thank Dr. Richard Howard, Timothy Bourett, and Keith Duncan for their excellent help with the confocal microscopy; Barbara Wiswall for baculovirus expression of Δ125MFP1; Dr. Albrecht von Arnim for the plasmid pRTL2–mGFPS65T; Dr. David Somers for a critical reading of the manuscript; and Dr. Udo Wienand for his support and for many fruitful discussions. This work was supported in part by a grant from the German Science Foundation (DFG) to I.M. (Grant No. ME 1133/2-1).

Received May 11, 1999; accepted June 13, 1999.

REFERENCES

Adams, M.D., et al. (1991). Complementary DNA sequencing: Expressed sequence tags and the human genome project. Science **252,** 1651–1656.

Allen, G.C., Hall, G., Jr., Michalowski, S., Newman, W., Spiker, S., Weissinger, A.K., and Thompson, W.F. (1996). High-level transgene expression in plant cells: Effects of a strong scaffold attachment region from tobacco. Plant Cell **8,** 899–913.

Altschul, S.F., Madden, T.L., Schaffer, A.A., Zhang, J., Zhang, Z., Miller, W., and Lipman, D.J. (1997). Gapped BLAST and PSI-BLAST: A new generation of protein database search programs. Nucleic Acids Res. **17,** 3389–3402.

Bartel, P., Chien, C.T., Sternglanz, R., and Fields, S. (1993). Elimination of false positives that arise in using the two-hybrid system. Biotechniques **6,** 920–924.

Berezney, R., and Coffey, D.S. (1974). Identification of a nuclear protein matrix. Biochem. Biophys. Res. Commun. **60,** 1410–1470.

Beven, A., Guan, Y., Pear, J., Cooper, C., and Shaw, P. (1991). Monoclonal antibodies to plant nuclear matrix reveal intermediate filament-related components within the nucleus. J. Mol. Biol. **228,** 41–57.

Boevink, P., Oparka, K., Santa Cruz, S., Martin, B., Betteridge, A., and Hawes, C. (1998). Stacks on tracks: The plant Golgi apparatus traffics on an actin/ER network. Plant J. **15,** 441–447.

Chevrier, V., Komesli, S., Schmitt, A.C., Vantard, M., Lambert, A.M., and Job, D. (1992). A monoclonal antibody, raised against mammalian centrosomes and screened by recognition of plant microtubule organizing centers, identifies a pericentriolar component in different cell types. J. Cell Sci. **101,** 823–835.

Chien, C.T., Bartel, P.L., Sternglanz, R., and Fields, S. (1991). The two-hybrid system: A method to identify and clone genes for proteins that interact with a protein of interest. Proc. Natl. Acad. Sci. USA **21,** 9578–9582.

Dellaporta, S.L., Wood, J., and Hicks, J.B. (1983). A plant DNA minipreparation: Version II. Plant Mol. Biol. Rep. **1,** 19–21.

Ellenberg, J., Siggia, E.D., Moreira, J.E., Smith, C.L., Presley, J.F., Worman, H.J., and Lippincott-Schwartz, J. (1997). Nuclear membrane dynamics and reassembly in living cells: Targeting of an inner nuclear membrane protein in interphase and mitosis. J. Cell Biol. **138,** 1193–1206.

Foisner, R., and Gerace, L. (1993). Integral membrane proteins of the nuclear envelope interact with lamins and chromosomes, and binding is modulated by mitotic phosphorylation. Cell **73,** 1267–1279.

Gant, T.M., and Wilson, K.L. (1997). Nuclear assembly. Annu. Rev. Cell Dev. Biol. **13,** 669–695.

Gindullis, F., and Meier, I. (1999). Matrix attachment region-binding protein MFP1 is localized in discrete domains at the nuclear envelope. Plant Cell **11,** 1117–1128.

Granado, R.R., Guoxun, L., Dersksen, A.C.G., and McKenna, K.A. (1994). A new insect cell line from *Trichoplusia ni* (BTI-Tn-5B1-4) susceptible to *Trichoplusia ni* single enveloped nuclear polyhedrosis virus. J. Invert. Pathol. **64,** 260–266.

Grebenok, R.J., Lambert, G.M., and Galbraith, D.W. (1997). Characterization of the targeted nuclear accumulation of GFP within the cells of transgenic plants. Plant J. **12,** 685–696.

Hall, G., Jr., Allen, G.S., Loer, D.S., Thompson, W.F., and Spiker, S. (1991). Nuclear scaffolds and scaffold-attachment regions in higher plants. Proc. Natl. Acad. Sci. USA **88,** 9320–9324.

Hein, J. (1990). Unified approach to alignment and phylogenies. Methods Enzymol. **183,** 626–645.

Iwabuchi, K., Li, B., Bartel, P., and Fields, S. (1993). Use of the two-hybrid system to identify the domain of p53 involved in oligomerization. Oncogene **6,** 1693–1696.

Luderus, M.E.E., de Graaf, A., Mattia, E., den Blaauwen, J.L., Grande, M.A., de Long, L., and van Driel, R. (1992). Binding of matrix attachment regions to lamin B_1. Cell **70,** 949–959.

Lutke, H.A., Chow, K.C., Mickel, F.S., Moos, K.A., Kern, H.F., and Scheele, G.A. (1987). Selection of AUG initiation codons differs in plants and animals. EMBO J. **6,** 43–48.

Masuda, K., Xu, Z.-J., Takahashi, S., Ito, A., Ono, M., Nomura, K., and Inoue, M. (1997). Peripheral framework of carrot cell nucleus contains a novel protein predicted to exhibit a long α-helical domain. Exp. Cell Res. **232,** 173–181.

McKeon, F.D., Kirschner, M.W., and Caput, D. (1986). Homologies in both primary and secondary structure between nuclear envelope and intermediate filament proteins. Nature **319,** 463–468.

McNulty, A.K., and Saunders, M.J. (1992). Purification and immunological detection of pea nuclear intermediate filaments: Evidence for plant nuclear lamins. J. Cell Sci. **103,** 407–414.

Meier, I., Phelan, T., Gruissem, W., Spiker, S., and Schneider, D. (1996). MFP1, a novel plant filament-like protein with affinity for matrix attachment region DNA. Plant Cell **8,** 2105–2115.

Mewes, H.W., Hani, J., Pfeiffer, F., and Frishman, D. (1998). MIPS: A database for protein sequences and complete genomes. Nucleic Acids Res. **26,** 33–37.

Minguez, A., and Moreno Diaz de la Espina, S. (1993). Immunological characterization of lamins in the nuclear matrix of onion cells. J. Cell Sci. **106,** 431–439.

Mirkovitch, J., Mirault, M.-E., and Laemmli, U.K. (1984). Organization of the higher-order chromatin loop: Specific DNA attachment sites on nuclear scaffolds. Cell **39,** 223–232.

Misteli, T., and Spector, D.L. (1998). The cellular organization of gene expression. Curr. Opin. Cell Biol. **10,** 323–331.

Nickerson, J.A., Blencowe, B.J., and Penman, S. (1995). The architectural organization of nuclear metabolism. Int. Rev. Cytol. **162A,** 67–123.

Nielsen, H., Engelbrecht, J., Brunak, S., and von Heijne, G. (1997). Identification of prokaryotic and eukaryotic signal peptides and prediction of their cleavage sites. Protein Eng. **10,** 1–6.

Restrepo-Hartwig, M.A., and Ahlquist, P. (1996). Brome mosaic virus helicase– and polymerase-like proteins colocalize on the endoplasmatic reticulum at sites of viral RNA synthesis. J. Virol. **70,** 8908–8916.

Sambrook, J., Fritsch, E.M., and Maniatis, T. (1989). Molecular Cloning: A Laboratory Manual. (Cold Spring Harbor, NY: Cold Spring Harbor Laboratory Press).

Schaad, M.C., Jensen, P.E., and Carrington, J.C. (1997). Formation of plant RNA virus replication complexes on membranes: Role of an endoplasmic reticulum–targeted viral protein. EMBO J. **16,** 4049–4059.

Schafer, W.R., and Rine, J. (1992). Protein prenylation: Genes, enzymes, targets and functions. Annu. Rev. Genet. **30,** 209–237.

Simos, G., and Georgatos, S.D. (1992). The inner nuclear membrane protein p58 associates in vivo with a p58 kinase and the nuclear lamins. EMBO J. **11,** 4027–4036.

Smith, H.M.S., and Raikhel, N.V. (1998). Nuclear localization signal receptor importin α associates with the cytoskeleton. Plant Cell **10,** 1791–1799.

Taniura, H., Glass, C., and Gerace, L. (1995). A chromatin binding site in the tail domain of nuclear lamins that interacts with histones. J. Cell Biol. **131,** 33–44.

Verheijnen, R., Van Venrooij, W., and Ramaekers, F. (1988). The nuclear matrix: Structure and composition. J. Cell Sci. **90,** 11–36.

von Arnim, A., Deng, X.W., and Stacey, M.G. (1998). Cloning vectors for the expression of green fluorescent protein fusion proteins in transgenic plants. Gene **221,** 35–43.

Wanner, L.A., and Gruissem, W. (1991). Expression dynamics of the tomato *rbcS* gene family during development. Plant Cell **3,** 1289–1303.

Watson, J.C., and Thompson, W.F. (1986). Purification and restriction endonuclease analysis of plant nuclear DNA. Methods Enzymol. **118,** 57–75.

Wei, X., Samarabandu, J., Devdhar, R.S., Siegel, A.J., Acharya, R., and Berezney, R. (1998). Segregation of transcription and replication sites into higher order domains. Science **281,** 1502–1505.